

# Materials Advances

Accepted Manuscript

This article can be cited before page numbers have been issued, to do this please use: S. Rafiq, N. Sultan and M. R. S. A. Janjua, *Mater. Adv.*, 2026, DOI: 10.1039/D6MA00220J.



This is an Accepted Manuscript, which has been through the Royal Society of Chemistry peer review process and has been accepted for publication.

Accepted Manuscripts are published online shortly after acceptance, before technical editing, formatting and proof reading. Using this free service, authors can make their results available to the community, in citable form, before we publish the edited article. We will replace this Accepted Manuscript with the edited and formatted Advance Article as soon as it is available.

You can find more information about Accepted Manuscripts in the [Information for Authors](#).

Please note that technical editing may introduce minor changes to the text and/or graphics, which may alter content. The journal's standard [Terms & Conditions](#) and the [Ethical guidelines](#) still apply. In no event shall the Royal Society of Chemistry be held responsible for any errors or omissions in this Accepted Manuscript or any consequences arising from the use of any information it contains.

# *In Silico* Design to Explore the Effect of Metalloporphyrin and C<sub>60</sub> Cage on the non-linear optical (NLO) Properties

Shama Rafiq<sup>1</sup>, Nimra Sultan<sup>1</sup> and Muhammad Ramzan Saeed Ashraf Janjua<sup>1,2\*</sup>

<sup>1</sup>Department of Chemistry, Government College University Faisalabad, Faisalabad 38000, Pakistan.

<sup>2</sup>Research Center for Crystal Materials, CAS Key Laboratory of Functional Materials and Devices for Special Environments, Xinjiang Technical Institute of Physics and Chemistry, CAS, 40-1 South Beijing Road, Urumqi, 830011, P.R. China

e-mail: [Janjua@gcuf.edu.pk](mailto:Janjua@gcuf.edu.pk) and [Dr\\_Janjua2010@yahoo.com](mailto:Dr_Janjua2010@yahoo.com) Cell: +92 300 660 49 48

## Abstract

The uses of nonlinear optical (NLO) materials in photonics, optoelectronics, optical switching, and data storage have drawn a lot of interest. This work provides a theoretical analysis of how Zn-porphyrin and fullerene (C<sub>60</sub>) cage affect the NLO characteristics of four designed systems: MP1, MP2, MP1C<sub>60</sub>, and MP2C<sub>60</sub>. To optimize molecular geometries and assess important parameters like HOMO-LUMO energy gaps, dipole polarizability, and first order hyperpolarizability, Density Functional Theory (DFT) calculations using the B3LYP functional were utilized. MP2 showed improved charge delocalization with the smallest energy gap (0.376 eV). Fullerene's function as an efficient electron acceptor was confirmed by functionalization with C<sub>60</sub>, which changed the electronic distributions in MP1C<sub>60</sub> and MP2C<sub>60</sub>. Structural stability was demonstrated by the Zn-N bond lengths remaining constant at 2.07 nm. Significant improvements were seen in polarizability and hyperpolarizability, especially for MP2C<sub>60</sub> ( $\beta_{total} = 78128.92 \times 10^{-30}$  esu). According to these results, metalloporphyrin and C<sub>60</sub> work in concert to significantly enhance NLO



performance, making these hybrids attractive options for cutting-edge photonic and optoelectronic applications.

**Keywords:** NLO; Metalloporphyrin; C<sub>60</sub> cage; DFT; HOMO-LUMO energy level; Polarizability; First order polarizability

## 1. Introduction

In recent decades, the scientific discipline of non-linear optics has experienced remarkable growth. It is predicated on the phenomenon of powerful coherent light radiation interacting with matter. The study of how light interacts with matter in situations where the atoms' non-linear response is significant is known as non-linear optics [1]. Organic compounds with NLO properties became unmatched in popularity and dominance in a variety of fields, including medicine, material science, atomic, molecular, and solid-state physics, surface interface sciences, and chemical dynamics, as a result of the quick development of high-tech electronic, optical, and storage devices [2,3]. Many materials, including graphene [4,5], fullerene [6], and quantum dots [7,8], have garnered scientific interest in recent decades due to their noteworthy nonlinear optical (NLO) characteristics. The study of organic and organometallic chromophores has also received a great deal of attention. In these cases, nonlinearity is primarily caused by the so-called push-pull architecture, which consists of a donor and an acceptor moiety connected by a  $\pi$ -delocalized spacer [9]. The NLO characteristics of the fundamental molecules dictate the NLO characteristics of the materials. Modeling organic molecules with high NLO characteristics is beneficial when using this criterion [10,11]. Appropriate donor- $\pi$ -spacer-acceptor (D- $\pi$ -A) systems with structurally modifiable features are required to model and build high-response NLO materials. In this way, substitution is a key component in the conjugation modification and, consequently, the NLO activity [12,13]. A lot of work has gone into getting very effective NLO materials. It is commonly recognized that altering the donor and acceptor capacities and prolonging the  $\pi$ -conjugated bridge can control the molecular second-order NLO characteristics. The electronic intramolecular charge transfer (ICT) of the molecule is linked to the initial hyperpolarizability and, consequently, the second-order NLO response [14,15].

Because of their structural diversity and ease of chemical alteration, porphyrins and metalloporphyrins are frequently employed as field-responsive materials in optoelectronics. Their ligands are useful for nonlinear optical applications because they offer significant dipole moments, polarizabilities, and hyperpolarizabilities. The potential of polymeric porphyrins in innovative



materials applications is increased by their remarkable low-dimensional conductivity [16]. Porphyrins have garnered a lot of interest as an organic material with an elevated nonlinear optical susceptibility in the hunt for better third-order nonlinearity materials because of their large p-electron system with 2D conjugated molecular arrangements as well as the presence of 1D delocalized electrons [17]. Because of their high solubility, probable processability as layers, and thermal and chemical durability, 2D structures based on delocalized macrocycles, including porphyrins and metal porphyrins, have garnered a lot of interest [18]. Furthermore, they can easily create an electronic exchange in a push-pull system by using their polarizable conjugated ring as a linker, which is necessary for a significant second order NLO response [19]. To create different donor-( $\pi$ -conjugated bridge)-acceptor (D- $\pi$ -A) and D- $\pi$ -D systems, porphyrins and metalloporphyrins can be utilized as  $\pi$ -conjugated bridges [20,21]. Previous research showed that metal complexation and the type of suitable donor-acceptor substituents can readily adjust the NLO characteristics of porphyrins [22-24].

A network of fused carbon atoms forms the spherical carbon cage known as fullerene molecules. Specifically, C<sub>60</sub> fullerene is made up of 60 carbon atoms organized in a highly symmetrical configuration [25]. Since buckminsterfullerene (C<sub>60</sub>) characterization, fullerenes and its derivatives have garnered a lot of attention due to their special physicochemical characteristics, which are helpful in a variety of material science applications [26-28]. The polyhedral counterparts of two-dimensional graphene sheets are called fullerenes. Though in trace proportions, they have been found in interplanetary space and are found in nature [29-31]. Because of its distinct physical and molecular characteristics, C<sub>60</sub> has garnered a lot of scientific attention [32]. The most significant features of C<sub>60</sub> are by far its extremely symmetric structure, its capacity for multiple addition processes, and its remarkable electron-accepting capabilities (e.g., it can take on up to six electrons) [33]. A number of the applications are still in their infancy, and fullerenes have only lately been employed in innovative optical applications, cancer therapy, and noninvasive cancer imaging. Future studies will examine the fullerene C<sub>60</sub>'s uses in catalysis, water purification, biohazard prevention, portable electricity, automobiles, and medicine [34].

Nanostructured thin films with tunable sizes enable charge carrier confinement, making them essential for optoelectronic applications [35]. Various advanced materials, including rare-earth-doped up-converting systems, polyoxometalates, metal nanoclusters, and cage-cluster frameworks, have been explored for nonlinear optical (NLO) applications due to their unique



optical and electronic properties, although some are limited by low efficiency or slow development [36-39]. In particular, Ag/Au nanoclusters and silver alkynyl systems exhibit strong quantum confinement and ultrafast response, making them promising for optoelectronics and all-optical switching [38,40]. Additionally, switchable NLO materials based on redox and photoresponsive mechanisms have gained attention for electro-optic applications [41]. Experimental studies, such as femtosecond Z-scan on TiO<sub>2</sub> nanoparticles, further confirm strong NLO responses, highlighting the broad potential of these materials in advanced photonic technologies [42].

We are now working to ascertain the hybrid composites' NLO responses to metalloporphyrin-C<sub>60</sub> cages. To put it briefly, we have theoretically created four hybrid composites using Zn-porphyrins and C<sub>60</sub> fullerenes in our research. We employed DFT calculations to forecast these composites' NLO response. In order to investigate the suggested molecules' NLO response, a number of metrics have been calculated, including linear polarizability, second-order nonlinearity, HOMO-LUMO gap, and charge transfer mechanism. For upcoming photonic and electronic devices, these hybrid materials might provide strong and adjustable NLO responses. The intelligent development of future optical materials can be guided by this method.

## 2. Computational Insights

The Gaussian 09 computational software is used to carry out the density functional theory (DFT) calculations [43]. Of the several DFT techniques that are available, we have chosen the B3LYP method [44], which combines the Lee, Yang, and Parr correlation functional (LYP) with Becke's three-parameter hybrid exchange functional (B3) [45]. In addition, B3LYP is accessible in the majority of quantum chemistry software packages and is quite simple to use [46]. Because of its accuracy in forecasting molecule structures and other properties, B3LYP is used in computational chemistry simulations in conjunction with the 6-311G basis set. Geometry optimization was performed using DFT theory at the B3LYP/6-31G\* level [47].

Finding the smallest point of energy is the aim of geometric optimization calculations since it represents the actual molecule structure and is used to compute bond length, bond angle, and other characteristics. The 6-311\*G was found to be appropriate for the atoms of H, O, and N [48]. While LANL2DZ (Los Alamos National Laboratory 2-double-z) associated with pseudo-potential was used for zinc (Zn). Selecting an appropriate model and calculation technique is essential for quantum chemical research in order to gather precise data and comprehend the connection between the computed outcomes and physical characteristics. The B3LYP approach is appropriate for



fullerene systems since several groups have used it and had satisfactory findings, and density functional theory is being utilized extensively in calculations because of its rather acceptable accuracy and affordable cost [49-51]. Additionally, the NLO properties of the optimized molecules had been taken into account. Using the same level of basis set and functional utilized for optimization, the first hyperpolarizabilities for each chemical system were found to determine the NLO characteristics. To further comprehend the charge transfer process in the investigated push-pull compounds, HOMO-LUMO analysis was also carried out.

First order polarizability and first-order hyperpolarizability were examined using an additional computational approach. The following formulas are used to determine hyperpolarizability  $\langle\beta\rangle$  and polarizability  $\langle\alpha\rangle$ . First order polarizability is computed using equation (1) [52].

$$\langle\alpha\rangle = 1/3(a_{xx} + a_{yy} + a_{zz}). \quad (1)$$

Whereas for the calculation of first order hyperpolarizability, we use the equation (2) [53].

$$\langle\beta\rangle = (\beta_x^2 + \beta_y^2 + \beta_z^2)^{1/2}$$

Where

$$\beta_x = \beta_{xxx} + \beta_{xyy} + \beta_{xzz}$$

$$\beta_y = \beta_{yyy} + \beta_{xxy} + \beta_{yzz}$$

$$\beta_z = \beta_{zzz} + \beta_{xxz} + \beta_{yyz}$$

$$\beta_{tot} = [(\beta_{xxx} + \beta_{xyy} + \beta_{xzz})^2 + (\beta_{yyy} + \beta_{xxy} + \beta_{yzz})^2 + (\beta_{zzz} + \beta_{xxz} + \beta_{yyz})^2]^{1/2} \quad (2)$$

For a deeper understanding of the process of nonlinear polarization, we first consider first order polarizability ( $\alpha$ ), which represents an estimate of the degree of linear polarization under the influence of an electrical field. We have calculated the values of the first order polarizability ( $\alpha$ ) components for each compound using the mathematical equation (1). The magnitude of first order hyperpolarizability is calculated using equation (2).

### 3. Geometric Structure

Based on the Zn-porphyrin (Zn-P) and carbon 60 cage shown in Figure 1, we have created four push-pull molecules (MP1, MP2, MP1C<sub>60</sub>, and MP2C<sub>60</sub>) using DFT insights. The optimized bond distances are provided in Table 1. The zinc porphyrin core that serves as the main light-harvesting donor is the foundation of these four systems. The efficiency of charge transfer from the donor to the fullerene acceptor can be predicted by methodically altering the linkers and peripheral groups [54].



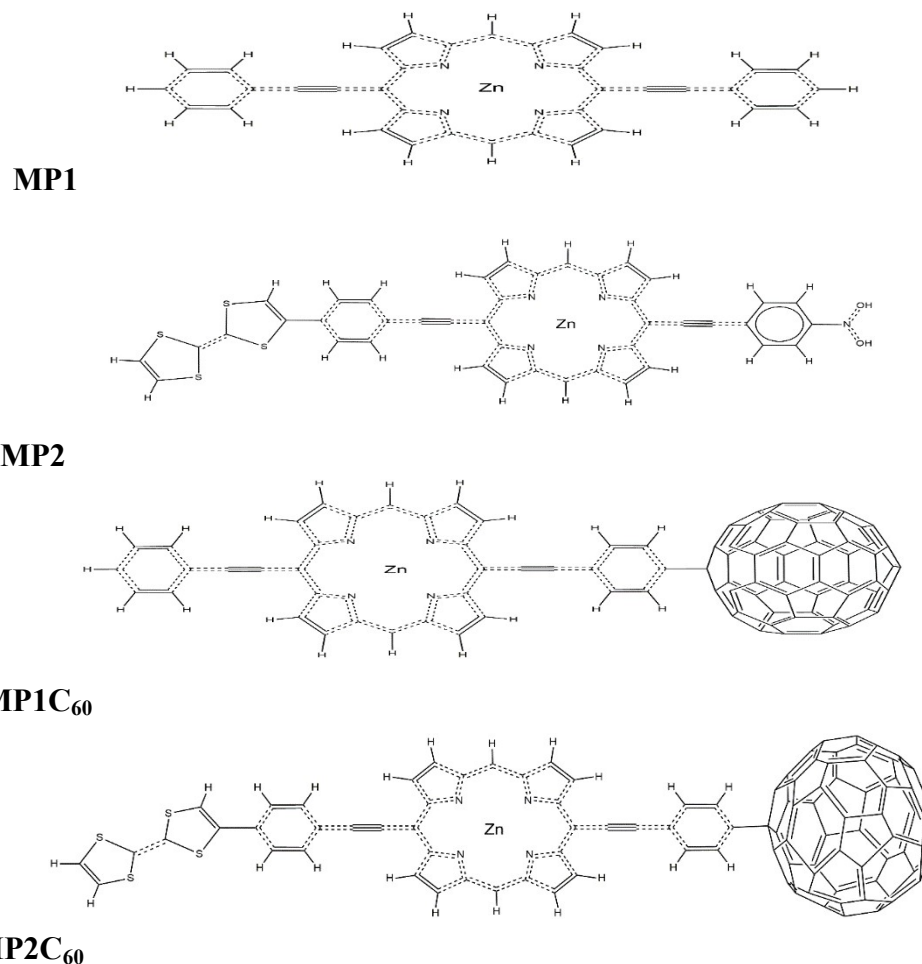


**Figure 1.** Chemical structures of the investigated systems: MP1, MP2, MP1C<sub>60</sub> and MP2C<sub>60</sub>.

**Table 1: Computed bond lengths in nm for all the four designed compounds**

Geometrical parameters	MPPP1	MPPP2	MPPP1C <sub>60</sub>	MPPP2C <sub>60</sub>
Zn-N	2.07 (2.0) *	2.07	2.07	2.07

We selected Zinc (Zn) porphyrin and Fullerene (C<sub>60</sub>) for their efficient donor-bridge-acceptor (D- $\pi$ -A) system, where a conjugated  $\pi$ -spacer facilitates rapid intramolecular charge transfer (ICT). This architecture promotes extensive electron redistribution under light, yielding high polarizability and enhanced second- and third-order hyperpolarizabilities, making the composite suitable for optical limiting, frequency modulation, and high-speed switching.

In MP1, there is a charge shift from Zn-porphyrin to the aromatic rings, indicating that the aromatic rings are acting as an electron attractor or acceptor and the Zn-porphyrin cage as an electron donor. TTF-based donor substituents that are affixed to the porphyrin framework in MP2



improve intramolecular charge transfer and electron-donating capacity. The aromatic rings serve as an electron donor for MP1C<sub>60</sub> and MP2C<sub>60</sub>, while the fullerene cage acts as an electron acceptor. Adding another fullerene to the opposite side of MP2C<sub>60</sub> would create a symmetric acceptor system, which could reduce directional intramolecular charge transfer (ICT) and partially lower nonlinear optical (NLO) efficiency. However, depending on conjugation and orbital alignment, it might enhance light absorption or stabilize excited states, so the overall NLO response would depend on molecular symmetry, orbital distribution, and electronic coupling.

When compared to porphyrin alone, the nonlinear optical (NLO) capabilities are greatly enhanced by the presence of fullerene. Although MP1C<sub>60</sub> is a small and effective model for quick electron transport, MP2C<sub>60</sub> functions as a more potent "molecular wire" thanks to its longer bridge. This MP2C<sub>60</sub> is intended to optimize the nonlinear optical response, thereby creating a more potent contender for laser protection and high-performance photonic devices.

#### 4. Results and Discussion

To investigate the NLO response of the suggested molecules, a few metrics were calculated, including linear polarizability, second order nonlinearity, HOMO-LUMO gap, and charge transfer mechanism. To characterize the chemical reactivity of the hybrid compounds, we have first described the HOMO-LUMO energy differential displayed in Fig. 2. All the compounds have smaller energy gaps, which suggests that there is a substantial charge transfer between the molecules. The easier the charge transfer, the smaller the energy gap between the HOMO and LUMO. Table 2 below shows the HOMO-LUMO energy differential.

**TABLE 2: Computed HOMO-LUMO energy difference (eV) for the designed molecules**

COMPOUND	MP1	MP2	MP1C <sub>60</sub>	MP2C <sub>60</sub>
E <sub>HOMO</sub> (eV)	-10.877	-9.369	-9.162	-8.220
E <sub>LUMO</sub> (eV)	-9.796	-8.933	-8.244	-7.507
$\Delta E = E_{LUMO} - E_{HOMO}$ (eV)	1.081	0.436	0.918	0.714

The designed molecules have HOMO energies between -10.877 and -8.220 eV and LUMO values between -9.796 and -7.507 eV. One crucial indicator of intramolecular charge transfer effectiveness and molecular electronic softness is the shrinking HOMO-LUMO energy gap. The magnitude of the electronic transmission between these units determines the bandgap. The non-

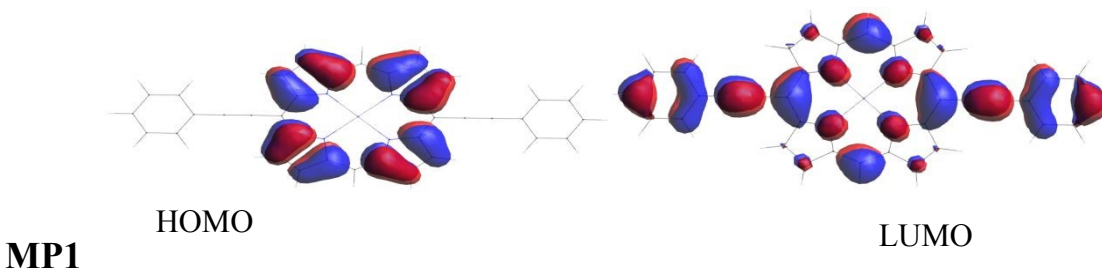


linear variation in gap values can be caused by various linkers, such as ethynylene-phenylene, which can either help or hinder this coupling. MP1 has the largest energy gap (1.081 eV) of any system under study, which suggests comparatively poorer electronic polarizability and charge transfer capacity. MP2, on the other hand, exhibits the lowest bandgap (0.436 eV), indicating better electronic delocalization and increased charge transport inside the molecular structure. MP2 has tetrathiafulvalene (TTF) derivatives (the sulfur-containing rings on the left), which contribute to the lower bandgap. Due to their minimal energy gap and intramolecular charge transfer (ICT), TTF derivatives are incredibly potent electron donors [55]. An extremely delocalized "electronic highway" can go throughout the entire molecule thanks to the structure of MP2. The "ground state" (HOMO) and "excited state" (LUMO) have very little energy difference when electrons are allowed to flow around a flat, conjugated system.

The complexes MP1C<sub>60</sub> and MP2C<sub>60</sub>, which include fullerene, have intermediary bandgap values that are 0.918 eV and 0.714 eV, respectively. As demonstrated in porphyrin-fullerene hybrid materials, where LUMO and HOMO are specifically localized on acceptor/donor parts of the molecule, the presence of an electron acceptor, such as fullerene, in D-A systems tunes frontier orbital energies and leads to charge transfer properties that affect nonlinear optical response [33]. Because of the steric barrier caused by the bulky fullerene's attachment, these complexes have a greater bandgap than MP2. By altering the orbitals' planar alignment and decreasing the effective conjugation, this crowding can distort the molecule structure and raise the HOMO-LUMO gap. Because MP2C<sub>60</sub> keeps the TTF-like donor groups from MP2, that are far more potent donors than the straightforward phenyl/alkyne groups in MP1C<sub>60</sub>, its bandgap is lower than MP1C<sub>60</sub>. Overall, the decreasing bandgap trend follows the order:

$$\text{MP1} > \text{MP1C}_{60} > \text{MP2C}_{60} > \text{MP2}$$

Figure 2 displays the chemical orbitals involved in these four molecules' main electron transitions.



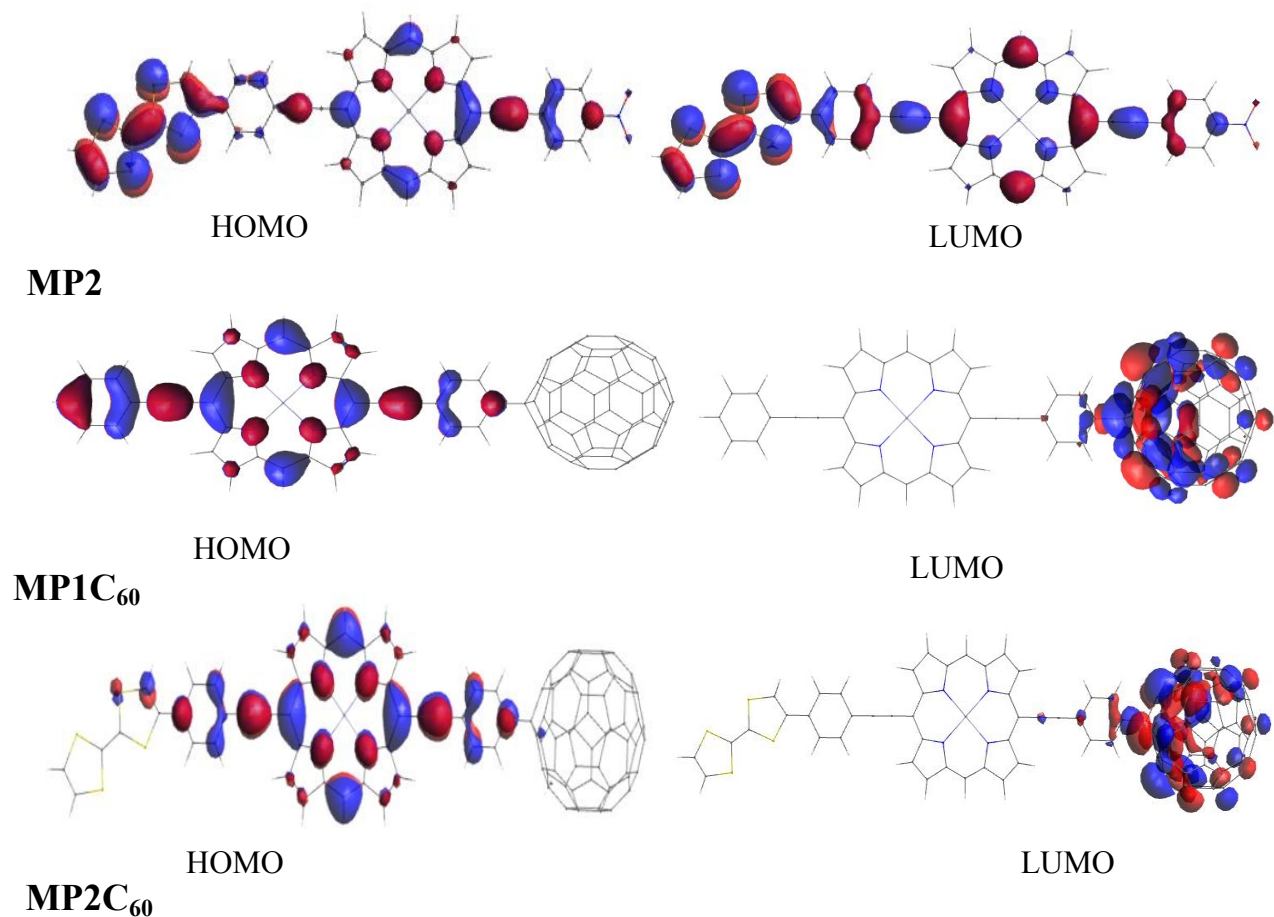


**Figure 2.** The frontier molecular orbitals of four designed molecules involved in the dominant electron transitions.

Examining the physical mechanism pertaining to the determination of the first order polarizability ( $a$ ) is equally crucial for the consideration of the first order hyperpolarizability ( $\beta$ ). First order polarizability is calculated using Equation 1. Table 2 shows the calculated dipole polarizability coefficients for four compounds.

**Table 3: First order polarizability elements (in  $1 \times 10^{-30}$  esu) for the four designed compounds**

Comp	$a_{xxx}$	$a_{yyy}$	$a_{zzz}$	$\langle a \rangle$
MP1	4.57	20.58	1.08	8.74
MP2	52.12	5.98	1.62	19.91
MP1C <sub>60</sub>	28.59	8.49	5.07	14.05



---

MP2C <sub>60</sub>	136.55	9.83	5.81	50.73
--------------------	--------	------	------	-------

---

The first order polarizability tensors  $a_{ii}$  ( $i = x, y, z$ ) for four chosen molecules are nonzero. According to the polarizability tensor study, MP2, MP1C<sub>60</sub>, and MP2C<sub>60</sub> show the highest polarizability along the x-axis, suggesting that the molecular backbone is where the majority of electron delocalization and charge transfer takes place. Conversely, MP1 exhibits more polarizability along the y-axis, indicating a distinct electron density distribution and much less longitudinal conjugation. Fullerene's attachment improves directional charge transfer along the x-axis because of its strong donor-acceptor interaction and extended  $\pi$ -conjugation.

The HOMO-LUMO bandgap and polarizability are typically inversely correlated in molecular systems [56]. Ahsin *et al.* (2024) establish that polaron formation in conducting polymers induces a significant reduction in the HOMO-LUMO energy bandgap ( $\Delta E$ ), resulting in a dramatic increase in the first hyperpolarizability ( $\beta$ ). This robust inverse relationship, where decreased excitation energy leads to enhanced nonlinear optical (NLO) response, shows  $\beta$  values increasing by up to 246 times in polaronic states [57]. An external electric field can more readily deform electrons with a smaller energy gap because they are less firmly attached to the nuclei. For example, MP2's average polarizability is 19.91 compared to 8.74, a direct result of its substantially shorter bandgap (0.436) than MP1's (1.081). Polarizability rises with molecular size and the degree of  $\pi$ -conjugation, according to structural analysis. By adding the big, electron-dense C<sub>60</sub> fullerene cage to the porphyrin structures, a vast reservoir of non-alignable electrons is created, which increases the first order polarizability values by "stretching" the electron cloud.

Electrons can move along the whole length of the TTF derivative, porphyrin, and fullerene units in long, linear molecules like the MP2C<sub>60</sub> triad. Adding groups like fullerenes can occasionally raise the bandgap by stabilizing the molecule's ground state, but first order polarizability is higher than that of all other compounds. Historically, the molecules have been divided into two categories: orbital controlled (soft-type) and charge controlled (hard-type). The soft-type relies on a molecule's capacity to transfer charge either instantly or permanently, whereas the hard-type relies on the molecule's uneven charge distribution. Due to their increased sensitivity to external perturbations, the border molecular orbitals are particularly implicated in soft-type interactions [58]. Despite having more electrons and being a bigger molecule, MP1C<sub>60</sub>'s bandgap (0.918 eV) is above double that of MP2 (0.436 eV). The increased excitation energy needed for



MP1C<sub>60</sub> produces a relatively stiff electron cloud that is less sensitive to an external electric field since polarizability and bandgap are negatively correlated. On the other hand, MP2's electron cloud is more flexible and easily polarizable due to its narrower bandgap, which makes electrical excitation simpler. As a result, MP1C<sub>60</sub> has a rather hard molecular nature with little electron cloud deformability, while MP2 has a softer molecular nature with better intramolecular charge transfer and increased polarizability. First order polarizability of four designed molecules decreases in following order.

$$\text{MP2C}_{60} > \text{MP2} > \text{MP1C}_{60} > \text{MP1}$$

Table 4 shows the total hyperpolarizability ( $\beta_{tot}$ ) and the calculated first-order hyperpolarizability tensor components ( $\beta_{xxx}$ ,  $\beta_{xxy}$ ,  $\beta_{xyy}$ , etc.) for MP1, MP2, MP1C<sub>60</sub>, and MP2C<sub>60</sub> by using equation 2.

**Table 4: Computed values of first order hyperpolarizability tensors ( $1 \times 10^{-30}$  esu) for all the compounds**

Tensors	MP1	MP2	MP1C <sub>60</sub>	MP2C <sub>60</sub>
$\beta_{xxx}$	0.00003917	-1418.692	-5702.829	78021.079
$\beta_{xxy}$	0.00070914	104.031	-10.591	-2395.119
$\beta_{xyy}$	-0.003496	28.205	-8.881	20.642
$\beta_{yyy}$	0.003226	2.266	0.538	10.432
$\beta_{xxz}$	0	-14.797	107.097	2315.702
$\beta_{yyz}$	0	-0.353	-1.787	-2.881
$\beta_{xzz}$	-0.00000339	-0.918	0.10038	16.416



$\beta_{yzz}$	0.000000332	0.0257	-0.752	-1.765
$\beta_{zzz}$	0	0.013	5.006	2.391
$\beta_{tot}$	0.00524	1395.54	5712.68	78128.92

Following order  $MP1 \ll MP2 < MP1C_{60} \ll MP2C_{60}$ , the calculated first-order hyperpolarizability ( $\beta_{tot}$ ) exhibits a noticeable increase across the systems under study. Because polarizability and first order hyperpolarizability reflect essentially different ways that molecules react to an electric field, their values do not follow the same upward trend. As molecules get longer from MP1 to MP2C<sub>60</sub>, polarizability ( $\alpha$ ), a linear property, increases proportionately with the molecular volume and total amount of electrons.

The first order hyperpolarizability, on the other hand, is a nonlinear feature that only depends on the extent of intramolecular charge transfer (ICT) and structural asymmetry. First order hyperpolarizability needs a "push-pull" system in which an electron-donating group is joined to an electron-accepting group by a conjugated bridge, whereas polarizability only needs room for electrons to move. Compared to systems incorporating fullerene, MP1 and MP2 exhibit reduced hyperpolarizability due to their stiffer electron clouds, absence of prolonged  $\pi$ -conjugation, and limited intramolecular charge transfer. The enhanced hyperpolarizability ( $\beta$ ) of MP2 relative to MP1, prior to fullerene attachment, arises from the presence of stronger electron-donating TTF derivative, which increase intramolecular charge transfer and extend  $\pi$ -conjugation within the molecular framework. The sulfur-containing rings improve electron delocalization and polarizability due to their higher electron density and polarizable nature, leading to greater charge separation under an applied electric field. In contrast, the phenyl groups in MP1 exhibit comparatively weaker electron-donating ability and limited conjugation efficiency. As a result, MP2 demonstrates a more pronounced nonlinear optical response than MP1 even before the incorporation of Fullerene C<sub>60</sub>, highlighting the intrinsic contribution of its molecular architecture to the observed increase in  $\beta$ .

C<sub>60</sub> is a common compound used in multicomponent molecular architecture to adjust its optical properties to certain spectral regions of interest because of its high electron-accepting capabilities and exceptionally small reorganization energy (ca. 0.23 eV). By employing chemical techniques, the average hyperpolarizabilities in fullerene derivatives are greatly enhanced by the C<sub>60</sub> moiety,



which functions as an electron acceptor in the ground electronic state [6]. The delocalization of charge from the electron-rich moiety to the electron-poor carbon cage, which results in partially negatively charged fullerene moieties, is primarily responsible for the observed increase. Chemical changes including a range of organic moieties that donate electrons have therefore been investigated [59]. Extended  $\pi$ -conjugation and a robust donor-acceptor (D-A) design cause the linear polarizability ( $\alpha$ ) and second-order hyperpolarizability ( $\beta$ ) to grow from MP1 to MP2C<sub>60</sub>. Due of its symmetric electronic distribution and large HOMO-LUMO gap ( $\Delta E$ ), which restricts excitation, MP1 exhibits the lowest NLO response. MP2C<sub>60</sub>, on the other hand, has a powerful push-pull mechanism that allows for intense intramolecular charge transfer (ICT) by using the TTF derivative as a strong donor and C<sub>60</sub> as a strong acceptor. A LUMO on the C<sub>60</sub> cage and a HOMO on the donor section are shown by FMO analysis. The two-state model states that MP2C<sub>60</sub>'s reduced bandgap improves the transition dipole and dipole change upon excitation, leading to better NLO performance.

By introducing a powerful electron-accepting unit, the fullerene attachment in MP1C<sub>60</sub> creates a donor-acceptor system that facilitates intramolecular charge transfer (ICT) from the donor backbone to the fullerene acceptor. The dominating  $\beta_{xxx}$  tensor component reflects the fullerene's ability to increase the  $\pi$ -conjugation length, which facilitates electron delocalization along the molecular axis. By lowering the excitation energy across the charge-transfer pathway, this prolonged conjugation and improved ICT cause  $\beta_{tot}$  to increase fourfold in comparison to MP2. The smaller  $\pi$ -conjugation pathway and poorer donor-acceptor strength of MP1C<sub>60</sub>'s molecular framework are the main causes of its lower initial hyperpolarizability when compared to MP2C<sub>60</sub>. MP2C<sub>60</sub> has a longer, electron-rich donor system that is connected to the C<sub>60</sub> electron-acceptor moiety which enables a much larger and more effective Intramolecular Charge Transfer (ICT). The first hyperpolarizability is a nonlinear property that increases exponentially with the distance from which electrons can be displaced. MP1C<sub>60</sub>'s shorter bridge and smaller donor moiety restrict the amount of electronic polarization, although having the same potent fullerene acceptor. As a result, MP2C<sub>60</sub> has a big  $\beta_{xxx}$  tensor component and a total  $\beta$  value that is more than thirteen times greater than that of MP1C<sub>60</sub>. This indicates both more structural asymmetry and greater electronic polarization due to enhanced intramolecular charge transfer. Overall, the remarkable improvement in hyperpolarizability for MP1C<sub>60</sub> and MP2C<sub>60</sub> is mostly caused by the addition of fullerene to these molecules, as well as ideal donor-acceptor geometries and prolonged conjugation. Of the



systems under study, MP2C<sub>60</sub> has the highest polarizability and hyperpolarizability, making it the most promising option for nonlinear optical applications as shown in Table 5.

**Table 5: HOMO-LUMO energies, bandgap, polarizability ( $\alpha$ ), and hyperpolarizability ( $\beta \times 10^{-30}$  esu) of MP1, MP2, MP1C<sub>60</sub>, and MP2C<sub>60</sub>.**

Comp	MP1	MP2	MP1C <sub>60</sub>	MP2C <sub>60</sub>
HOMO (eV)	-10.877	-9.369	-9.162	-8.220
LUMO (eV)	-9.796	-8.933	-8.244	-7.507
Bandgap (eV)	1.081	0.436	0.918	0.714
Polarizability ( $\alpha$ ) ( $1 \times 10^{-30}$ esu)	8.74	19.91	14.05	50.73
Hyperpolarizability ( $\beta$ ) ( $1 \times 10^{-30}$ esu)	0.00524	1395.54	5712.68	78128.92

The reported NLO coefficients are theoretically calculated using DFT/TD-DFT methods, and no experimental measurements have been performed; experimental verification is suggested as future work. However the suggested Zn porphyrin-bridge-fullerene molecules can be produced by attaching stiff ethynyl spacers and thiophene units to the porphyrin core by well-known palladium-catalyzed cross-coupling processes, such as Sonogashira or Suzuki reactions. The carbon cage can then be precisely functionalized by covalently joining the fullerene (C<sub>60</sub>) moiety by high-yield "click-like" reactions like the Bingel reaction or the Prato reaction. The conjugation length and donor-acceptor distance, which are critical for adjusting the nonlinear optical (NLO) characteristics and guaranteeing the stability of the finished composite, can be precisely controlled using these modular synthetic approaches.

In a related study, the first-order hyperpolarizability ( $\beta$ ) of para-aminobenzoic acid is  $29.99 \times 10^{-30}$  esu, indicating moderate nonlinear optical (NLO) behavior [60]. In contrast, the MP2C<sub>60</sub> system exhibits a significantly higher  $\beta$  of  $78128.92 \times 10^{-30}$  esu an enhancement of approximately 2600-fold due to strong intramolecular charge transfer, extended  $\pi$ -conjugation, and a smaller band gap (0.714 eV). Urea-barbituric acid (UBA) crystals that have been investigated experimentally exhibit significant third-order NLO activity and effective optical limiting, but their high band gap ( $\sim 4.50$  eV) restricts charge transfer, decreasing first-order hyperpolarizability [61]. Excellent third-order NLO capabilities are also displayed by morphology-dependent MoS<sub>2</sub> nanoplatelets, which have a low optical limiting threshold ( $0.73 \times 10^{12}$  W/m<sup>2</sup>) and a high nonlinear absorption



coefficient ( $5.9 \times 10^{-10}$  m/W) [62]. Overall, UBA and MoS<sub>2</sub> are very successful in third-order nonlinear absorption-based optical limiting, highlighting distinct NLO regimes, but MP2C<sub>60</sub> is superior in second-order NLO response.

## Conclusion

Bandgaps, polarizabilities, and first order hyperpolarizabilities of MP1, MP2, MP1C<sub>60</sub>, and MP2C<sub>60</sub> were used to study their NLO characteristics. Because of its stiff electron cloud and little intramolecular charge transfer, MP1 exhibits the highest bandgap and minimum polarizability, leading to negligible hyperpolarizability. MP2, which has a moderate polarizability and a narrower bandgap, shows a notable rise in  $\beta$  because of higher electron delocalization and donor-acceptor alignment. NLO responsiveness is significantly improved by fullerene connection in MP1C<sub>60</sub> and MP2C<sub>60</sub>. Extended  $\pi$ -conjugation and fullerene-induced charge transfer cause MP1C<sub>60</sub> to exhibit higher  $\beta$ , whereas excellent donor-acceptor geometry, extended conjugation, and greatly delocalized electrons cause MP2C<sub>60</sub> to exhibit the highest  $\beta$ . These findings demonstrate that while bandgap affects NLO behavior, the main determinants of first order hyperpolarizability are charge-transfer efficiency, conjugation duration, and molecule structure, which makes MP2C<sub>60</sub> an extremely interesting option for nonlinear optical uses.

## Acknowledgements

The authors acknowledge the support provided by the President's International Fellowship Initiative (PIFI) Project No. 2024VEA0015 of the Chinese Academy of Sciences (CAS).

## References

1. Suresh, S., Ramanand, A., Jayaraman, D., & Mani, P. (2012). Review on theoretical aspect of nonlinear optics. *Rev. Adv. Mater. Sci*, 30(2), 175-183.
2. Khan, M. U., Khalid, M., Asim, S., Momina, Hussain, R., Mahmood, K., ... & Lu, C. (2021). Exploration of nonlinear optical properties of triphenylamine-dicyanovinylene coexisting donor- $\pi$ -acceptor architecture by the modification of  $\pi$ -conjugated linker. *Frontiers in Materials*, 8, 719971.
3. Christodoulides, D. N., Khoo, I. C., Salamo, G. J., Stegeman, G. I., & Van Stryland, E. W. (2010). Nonlinear refraction and absorption: mechanisms and magnitudes. *Advances in Optics and Photonics*, 2(1), 60-200.
4. Kumar, V. (2021). Linear and Nonlinear Optical Properties of Graphene: A Review. *Journal of Electronic Materials*, 50(7).



5. You, J. W., Bongu, S. R., Bao, Q., & Panoiu, N. C. (2018). Nonlinear optical properties and applications of 2D materials: theoretical and experimental aspects. *Nanophotonics*, 8(1), 63-97.
6. Loboda, O., Zalesny, R., Avramopoulos, A., Luis, J. M., Kirtman, B., Tagmatarchis, N., ... & Papadopoulos, M. G. (2009). Linear and nonlinear optical properties of [60] fullerene derivatives. *The Journal of Physical Chemistry A*, 113(6), 1159-1170.
7. Limosani, F., Carcione, R., & Antolini, F. (2020). Formation of CdSe quantum dots from single source precursor obtained by thermal and laser treatment. *Journal of Vacuum Science & Technology B*, 38(1).
8. Antolini, F., Limosani, F., & Carcione, R. (2022). Direct Laser Patterning of CdTe QDs and Their Optical Properties Control through Laser Parameters. *Nanomaterials*, 12(9), 1551.
9. Limosani, F., Tessore, F., Forni, A., Lembo, A., Di Carlo, G., Albanese, C., ... & Tagliatesta, P. (2023). Nonlinear Optical Properties of Zn (II) Porphyrin, Graphene Nanoplates, and Ferrocene Hybrid Materials. *Materials*, 16(15), 5427.
10. Garza, A. J., Osman, O. I., Wazzan, N. A., Khan, S. B., Asiri, A. M., & Scuseria, G. E. (2014). A computational study of the nonlinear optical properties of carbazole derivatives: theory refines experiment. *Theoretical Chemistry Accounts*, 133(4), 1458.
11. Zhong, R. L., Sun, S. L., Xu, H. L., Qiu, Y. Q., & Su, Z. M. (2014). Helical carbon segment in carbon–boron–nitride heteronanotubes: structure and nonlinear optical properties. *ChemPlusChem*, 79(5), 732-736.
12. Janjua, M. R. S. A. (2017). Nonlinear optical response of a series of small molecules: quantum modification of  $\pi$ -spacer and acceptor. *Journal of the Iranian Chemical Society*, 14(9), 2041-2054.
13. Janjua, M. R. S. A., Yamani, Z. H., Jamil, S., Mahmood, A., Ahmad, I., Haroon, M., ... & Pan, S. (2016). First principle study of electronic and non-linear optical (NLO) properties of triphenylamine dyes: interactive design computation of new NLO compounds. *Australian Journal of Chemistry*, 69(4), 467-472.
14. Janjua, M. R. S. A., Mahmood, A., Nazar, M. F., Yang, Z., & Pan, S. (2014). Electronic absorption spectra and nonlinear optical properties of ruthenium acetylide complexes: a DFT study toward the designing of new high NLO response compounds. *Acta Chimica Slovenica*, 61(2).



15. Siddiqui, S. A., Rasheed, T., Faisal, M., Pandey, A. K., & Khan, S. B. (2012). Electronic structure, nonlinear optical properties, and vibrational analysis of gemifloxacin by density functional theory. *Journal of Spectroscopy*, 27(3), 185-206.
16. Chou, J. H., Kosal, M. E., Nalwa, H. S., Rakow, N. A., & Suslick, K. S. (2000). Applications of porphyrins and metalloporphyrins to materials chemistry. *The porphyrin handbook*, 6, 43-131.
17. Yan, L. K., Pomogaeva, A., Gu, F. L., & Aoki, Y. (2010). Theoretical study on nonlinear optical properties of metalloporphyrin using elongation method. *Theoretical Chemistry Accounts*, 125(3), 511-520.
18. Pizzotti, M., Annoni, E., Ugo, R., Bruni, S., Quici, S., Fantucci, P., ... & Zoppo, M. D. (2004). A multitechnique investigation of the second order NLO response of a 10, 20-diphenylporphyrinato nickel (II) complex carrying a phenylethynyl based push-pull system in the 5-and 15-positions. *Journal of Porphyrins and Phthalocyanines*, 8(11), 1311-1324.
19. Tessore, F., Orbelli Biroli, A., Di Carlo, G., & Pizzotti, M. (2018). Porphyrins for second order nonlinear optics (NLO): an intriguing history §. *Inorganics*, 6(3), 81.
20. Nayak, A., Park, J., De Mey, K., Hu, X., Duncan, T. V., Beratan, D. N., ... & Therien, M. J. (2016). Large hyperpolarizabilities at telecommunication-relevant wavelengths in donor–acceptor–donor nonlinear optical chromophores. *ACS Central Science*, 2(12), 954-966.
21. Koszelewski, D., Nowak-Król, A., Drobizhev, M., Wilson, C. J., Haley, J. E., Cooper, T. M., ... & Gryko, D. T. (2013). Synthesis and linear and nonlinear optical properties of low-melting  $\pi$ -extended porphyrins. *Journal of Materials Chemistry C*, 1(10), 2044-2053.
22. Hou, N., Liu, T. T., & Fang, X. H. (2023). A comparative study on nonlinear optical properties of zinc porphyrins analogs: Coordination atoms and group effects. *International Journal of Quantum Chemistry*, 123(11), e27104.
23. Di Carlo, G., Pizzotti, M., Righetto, S., Forni, A., & Tessore, F. (2020). Electric-field-induced second harmonic generation nonlinear optic response of A4  $\beta$ -pyrrolic-substituted ZnII porphyrins: When cubic contributions cannot be neglected. *Inorganic Chemistry*, 59(11), 7561-7570.
24. Islam, N., & Chimni, S. S. (2017). Geometrical structure and nonlinear response variations of metal (M= Ni<sup>2+</sup>, Pd<sup>2+</sup>, Pt<sup>2+</sup>) octaphyrin complex derivatives: A DFT study. *Journal of Coordination Chemistry*, 70(7), 1221-1236.



25. Aziz, M. T., Gill, W. A., Khosa, M. K., Jamil, S., & Janjua, M. R. S. A. (2024). Adsorption of molecular hydrogen (H<sub>2</sub>) on a fullerene (C<sub>60</sub>) surface: insights from density functional theory and molecular dynamics simulation. *RSC advances*, 14(49), 36546-36556.
26. Camacho Gonzalez, J., Mondal, S., Ocayo, F., Guajardo-Maturana, R., & Muñoz-Castro, A. (2020). Nature of C<sub>60</sub> and C<sub>70</sub> fullerene encapsulation in a porphyrin-and metalloporphyrin-based cage: Insights from dispersion-corrected density functional theory calculations. *International Journal of Quantum Chemistry*, 120(3), e26080.
27. Sheka, E. F. (2011). Fullerene nanoscience: nanochemistry, nanomedicine, nanophotonics, nanomagnetism. *CRC, Boca Raton*.
28. Hirsch, A., & Brettreich, M. (2006). *Fullerenes: chemistry and reactions*. John Wiley & Sons.
29. Schwerdtfeger, P., Wirz, L. N., & Avery, J. (2015). The topology of fullerenes. *Wiley Interdisciplinary Reviews: Computational Molecular Science*, 5(1), 96-145.
30. Berné, O., & Tielens, A. G. (2012). Formation of buckminsterfullerene (C<sub>60</sub>) in interstellar space. *Proceedings of the National Academy of Sciences*, 109(2), 401-406.
31. Cami, J., Bernard-Salas, J., Peeters, E., & Malek, S. E. (2010). Detection of C<sub>60</sub> and C<sub>70</sub> in a young planetary nebula. *Science*, 329(5996), 1180-1182.
32. Signorini, R., Bozio, R., & Prato, M. (2002). Optical limiting applications. In *Fullerenes: from synthesis to optoelectronic properties* (pp. 295-326). Dordrecht: Springer Netherlands.
33. Echegoyen, L. U. I. S., Diederich, F. R. A. N. Ç. O. I. S., & Echegoyen, L. E. (2000). *Electrochemistry of fullerenes* (pp. 1-51). John Wiley & Sons, Inc.: New York.
34. Shanbogh, P. P., & Sundaram, N. G. (2015). Fullerenes revisited: Materials chemistry and applications of C<sub>60</sub> molecules. *Resonance*, 20(2), 123-135.
35. Das, S., Alagarasan, D., Varadharajaperumal, S., Ganesan, R., & Naik, R. (2022). Tuning the nonlinear susceptibility and linear parameters upon annealing Ag<sub>60-x</sub>Se<sub>40</sub>Te<sub>x</sub> nanostructured films for nonlinear and photonic applications. *Materials Advances*, 3(20), 7640-7654.)
36. Ngo, T. T., Lozano, G., & Míguez, H. (2022). Enhanced up-conversion photoluminescence in fluoride–oxyfluoride nanophosphor films by embedding gold nanoparticles. *Materials Advances*, 3(10), 4235-4242.)
37. Deng, W., Zhu, Z., Sun, Y., Xu, H., Liu, S., & Wen, H. (2024). Recent advances in {P 4 Mo 6}-based polyoxometalates. *Polyoxometalates*, 3(4), 9140071.



38. Sanwal, P., Raza, A., Miao, Y. X., Lumbers, B., & Li, G. (2024). Advances in coinage metal nanoclusters: From synthesis strategies to electrocatalytic performance. *Polyoxometalates*, 3(3), 9140057.
39. Chen, R. Y., He, Y. P., & Zhang, J. (2022). Combining Ti4 (embonate) 6 cages and [Pb4 (OH) 4] 4+ clusters for enhanced third-order nonlinear optical property. *Polyoxometalates*, 1(1), 9140002.
40. Zhou, K., Yan, L. K., Geng, Y., Ji, J. Y., Wang, X. L., Su, Z. M., & Xiao, Z. G. (2021). The interesting luminescence behavior and rare nonlinear optical properties of the {Ag 55 Mo 6} nanocluster. *RSC advances*, 11(61), 38814-38819.
41. Ma, T. Y., Zhang, T., Zhu, B., Yan, L. K., & Su, Z. M. (2016). Theoretical studies on oxidation-switchable second-order nonlinear optical responses of Metallosalen-Keggin polyoxometalate derivatives. *RSC advances*, 6(58), 53438-53443.
42. Rana, A., Pathak, S., Kumar, K., Kumari, A., Chopra, S., Kumar, M., ... & Sharma, S. N. (2024). Multifaceted properties of TiO 2 nanoparticles synthesized using *Mangifera indica* and *Azadirachta indica* plant extracts: antimicrobial, antioxidant, and non-linear optical activity investigation for sustainable agricultural applications. *Materials Advances*, 5(7), 2767-2784.
43. Frisch MJ, Trucks GW, Schlegel HB, Scuseria GE, Robb MA, Cheeseman JR, et al. Gaussian 09, Revision D.01. Wallingford (CT): Gaussian, Inc.; 2013.
44. Halim, S. A., Ibrahim, M. A., Roushdy, N., Farag, A. A. M., Gabr, Y., & Said, S. (2018). Spectroscopic and TD-DFT investigations of 4-[(2-amino-6-methylchromon-3-yl) methylidene] amino}-6-methyl-3-thioxo-3, 4-dihydro-1, 2, 4-triazin-5 (2H)-one, and its application for photovoltaic devices. *Materials Chemistry and Physics*, 217, 403-411.
45. Farag, A. A. M., Roushdy, N., Halim, S. A., El-Gohary, N. M., Ibrahim, M. A., & Said, S. (2018). Synthesis, molecular, electronic structure, linear and non-linear optical and phototransient properties of 8-methyl-1, 2-dihydro-4H-chromeno [2, 3-b] quinoline-4, 6 (3H)-dione (MDCQD): Experimental and DFT investigations. *Spectrochimica Acta Part A: Molecular and Biomolecular Spectroscopy*, 191, 478-490.
46. Al-Otaibi, J. S., Mary, Y. S., Mary, Y. S., Krátký, M., Vinsova, J., & Gamberini, M. C. (2023). DFT, TD-DFT and SERS analysis of a bioactive benzohydrazide's adsorption in silver hydrosols at various concentrations. *Journal of Molecular Liquids*, 373, 121243.



47. El-Saady, A. A., Roushdy, N., Farag, A. A. M., El-Nahass, M. M., & Abdel Basset, D. M. (2023). Exploring the molecular spectroscopic and electronic characterization of nanocrystalline Metal-free phthalocyanine: a DFT investigation. *Optical and Quantum Electronics*, 55(7), 662.
48. Haroon, M. & Janjua, M. R. S. A. (2022). Computationally assisted design and prediction of remarkably boosted NLO response of organoimido-substituted hexamolybdates. *Journal of Physical Organic Chemistry*, 35: e4353.
49. Liu, S., Gao, F. W., Xu, H. L., & Su, Z. M. (2019). Transition metals doped fullerenes: structures–NLO property relationships. *Molecular Physics*, 117(6), 705-711.
50. Gao, F. W., Zhong, R. L., Sun, S. L., Xu, H. L., Zhao, L., & Su, Z. M. (2015). Charge transfer and first hyperpolarizability: cage-like radicals C59X and lithium encapsulated Li@ C59X (X= B, N). *Journal of molecular modeling*, 21(10), 258.
51. Wang, L. J., Zhong, R. L., Sun, S. L., Xu, H. L., Pan, X. M., & Su, Z. M. (2014). The V-shaped polar molecules encapsulated into C<sub>s</sub> (10528)-C<sub>72</sub>: stability and nonlinear optical response. *Dalton Transactions*, 43(25), 9655-9660.
52. Karakas, A., Elmali, A., & Unver, H. (2007). Linear optical transmission measurements and computational study of linear polarizabilities, first hyperpolarizabilities of a dinuclear iron (III) complex. *Spectrochimica Acta Part A: Molecular and Biomolecular Spectroscopy*, 68(3), 567-572.
53. Halim, S. A., & Ibrahim, M. A. (2022). Synthesis, spectral analysis, quantum studies, NLO, and thermodynamic properties of the novel 5-(6-hydroxy-4-methoxy-1-benzofuran-5-ylcarbonyl)-6-amino-3-methyl-1H-pyrazolo [3, 4-b] pyridine (HMBPP). *RSC advances*, 12(21), 13135-13153.
54. Liang, C., Cui, X., Dong, W., Qin, J., & Duan, Q. (2022). Enhanced non-linear optical properties of porphyrin-based polymers covalently functionalized with graphite phase carbon nitride. *Frontiers in Chemistry*, 10, 1102666.
55. Kamli, D., Hannachi, D., Samsar, D., & Chermette, H. (2023). Bis-TTF-Ge derivatives: promising linear and nonlinear optical properties, a theoretical investigation. *New Journal of Chemistry*, 47(3), 1234-1246.
56. Zhao, D., He, X., Ayers, P. W., & Liu, S. (2023). Excited-state polarizabilities: a combined density functional theory and information-theoretic approach study. *Molecules*, 28(6), 2576.



57. Ahsin, A., Ejaz, I., Sarfaraz, S., Ayub, K., & Ma, H. (2024). Polaron formation in conducting polymers: a novel approach to designing materials with a larger NLO response. *ACS omega*, 9(12), 14043-14053.
58. Macchi, P. (2025). Polarizabilities of Atoms in Molecules: Choice of the Partitioning Scheme and Applications for Secondary Interactions. *Molecules*, 30(20), 4137.
59. Limosani, F., Tessore, F., Di Carlo, G., Forni, A., & Tagliatesta, P. (2021). Nonlinear optical properties of porphyrin, fullerene and ferrocene hybrid materials. *Materials*, 14(16), 4404.
60. Lakhera, S., Rana, M., Devlal, K., Sharma, S., Chowdhury, P., Dhuliya, V., ... & Girisun, T. S. (2023). Exploring the nonlinear optical limiting activity of para-aminobenzoic acid by experimental and DFT approach. *Journal of Photochemistry and Photobiology A: Chemistry*, 444, 114987.
61. Suresh, A., Jauhar, R. M., Girisun, T. S., Manikandan, N., & Vinitha, G. (2024). Third order nonlinearity examined by pulsed and CW lasers: an organic urea barbituric acid (UBA) single crystal for optical limiting application with DFT study. *Materials Research Express*, 11(1), 016203.
62. Durairaj, M., TC, S. G., & Al-Sehemi, A. G. (2022). Impact of morphology on the nonlinear optical absorption of pristine molybdenum disulfide (MoS<sub>2</sub>) nanostructures. *Optical Materials*, 131, 112632.



The data that support the findings of this study are available from the corresponding author via email.

[View Article Online](#)  
DOI: 10.1039/D6MA00220J

